JOURNAL OF MATERIALS SCIENCE 32 (1997) 2921–2927

Hollow-shell formation – an important mode in the hydration of Portland cement

K. O. KJELLSEN, B. LAGERBLAD
Swedish Cement and Concrete Research Institute, 100 44 Stockholm, Sweden

H. M. JENNINGS
Department of Civil Engineering and Department of Materials Science and Engineering, Northwestern University, Evanston, ILL 60201, USA

The characteristics and quantities of hollow shells (Hadley grains) in the microstructure of Portland cement paste have been studied. It is shown that at relatively early hydration stages, the hydration largely occurs in a manner resulting in hollow shells. At later ages, the ''hollow-shell hydration'' mode becomes much less prominent as ''inner products'' are increasingly formed. The intrinsic porosity associated with hollow shells can be significant at later ages, between about 1% and 9%, depending on the mix composition and curing regime. The presence of silica fume increases the amount of hollow-shell porosity considerably, while the hollow-shell porosity appears to decrease with decreasing water/binder ratio.

1. Introduction

It is important to understand the mechanisms of cement hydration because it determines the intrinsic pore structure which, in turn, decisively influences many engineering properties. Early hydration models [1, 2] predict that the reaction products formed during cement hydration are deposited both inside the original cement grain boundary ("inner" product) and outside in the original water-filled space between the cement grains ("outer" product). Powers [2] stated that half of the products formed during hydration were deposited inside the boundaries of the original cement grain, while simultaneously, the other half of the reaction products would be deposited outside. Taplin [1] hypothesized that there was a coherent contact between the inner hydration products and the hydrating cement grains. The model was explained in terms of diffusion processes. The inner products may be formed by an *in situ* solid-state reaction. The outer products would be formed from dissolved species which diffuse through both inner and outer products and finally precipitate outside the original clinker boundaries, i.e. in the capillary pore space as defined by Verbeck [3].

Recently, several attempts have been made to classify the microstructural features found in cement paste. Diamond [4] suggested four types based on the morphology of fracture surfaces. The concept of "inner" and "outer" products has been modified as "early" and "late" [5] products, with the boundary between dense product and open product being not the surface of the original particle, but rather the surface of the anhydrous particle after some hours of reaction. Diamond and Bonen [6] have suggested a two-structure phenograin, or dense material, including C–S–H, CH and anhydrous grains. Finally, the idea of hollow-shell hydration has been suggested. In other words, voids can exist between unreacted grains and product.

Outer products may form while stable inner products may not form [7–14]. This results in progressively larger void space within a "shell" of outer products, i.e. within the original cement grain boundary. These voids, i.e. pseudoforms of clinker grains, are termed "hollow shells", or Hadley grains, after the discoverer [7]. They may be completely hollow, or they may be partially hollow. In a previous paper [14], we showed that hollow shells are true and common features of the microstructure; they are not artefacts of specimen preparation. Although our investigation is limited to a low-alkali sulphate-resistant cement, previous observations of hollow shells have been made on other types of Portland cements indicating that "hollow-shell hydration" is a significant mode of cement hydration, see, for example, [13]. In the present paper, we provide further experimental results that support this theory in the case of low-alkali sulphate-resistant Portland cement.

2. Experimental procedure

2.1. Materials

Paste specimens were made of Portland cement, condensed silica fume (csf), deionized water and a superplasticizer. The cement was a Swedish low-alkali sulphate-resistant cement (ASTM Type V) with chemical composition (weight per cent) 22.2% SiO_2, 3.4% Al_2O_3, 4.8% Fe_2O_3, 64.9% CaO, 0.91% MgO, 0.56%

TABLE I The material combinations studied. The numbers denoting mix combinations are the amount of superplasticizer (%)

csf (%)	Water/binder ratio			
	0.25	0.30	0.40	0.55
0	3.0	–	0.5	0
5	–	2.0	–	–
10	4.0	–	1.5	–

K_2O, 0.04% Na_2O, 2.0% SO_3, 0.63% ignition loss. The Blaine specific surface area and density were 302 $m^2 kg^{-1}$ and 3220 $kg m^{-3}$, respectively. The Bogue composition was 19.8% C_2S, 58.1% C_3S, 0.8% C_3A, 14.5% C_4AF. The csf contained 94.2% SiO_2, had a loss-on-ignition of 1.8%, a specific surface area of 23.0 $m^2 g^{-1}$ and a density of 2328 $kg m^{-3}$. The csf was in slurry form and contained 50% solids. The plasticizer was composed of 40% sulphonated naphthalene formaldehyde, 0.3% tributyl phosphate, and water. The water/binder ratio (w/b) ranged from 0.25–0.55, thus covering the cement paste phase of high-performance concrete, as well as conventional concrete. The binder contained either 0%, 5%, or 10% csf by weight. The material matrix is shown in Table I. The percentage of plasticizer (per cent) of the binder weight is given in Table I and only the denoted combinations were made.

The materials were chilled to about 15 °C before mixing. The ingredients were thoroughly mixed first in a Hobart mixer and then for a short period by a high-speed dispersion blender. The fresh paste temperature was about 20 °C and subsequent curing took place at 20 °C. The detailed mixing procedure ensured a smooth paste with well dispersed csf. The paste was cast in moulds with 12 mm cube compartments; the moulds were completely sealed and rotated under water for at least 12 h in order to prevent segregation of the paste before the forms were opened. The specimens were then placed in tight glass bottles. This ensured sealed curing conditions with practically no moisture exchange or carbonation. Specimens were generally tested at 12 h, 1, 28 and 91 d, and 9 mon. Note that specimens of the 0.30 w/b ratio paste were cured in two ways; one set of specimens was cured under sealed conditions, while the other was submerged in a small volume of water from 28 d to 9 mon. Carbonation was avoided.

2.2. Methods and specimen preparation

Polished epoxy-impregnated specimens were examined in an SEM, operated at an accelerating voltage of 10 kV and the working distance was 15 mm. Details of the specimen preparation procedure may be found elsewhere [15]. X-ray microanalyses were performed in order to identify various phases. A detailed quantitative EDX investigation of the specimens studied in the present work will be reported at a later stage [16].

Back-scattered electron (BSE) images were obtained for image analysis. The beam current was held constant at 1.5 nA, as measured in a Faraday cup. Monitor images (CRT) were obtained at a magnification of x400 and were transformed to binary images of 1024 x 1024 pixels. This provided a pixel size corresponding to about 0.25 μm across. The signal-to-noise ratio was improved by acquiring the binary image three times at a slow scan speed and averaging. Eight areas were analysed for each specimen, giving a total area of approximately 0.5 mm^2. The contrast and brightness measured on the waveform monitor of the microscope was corrected manually and held as constant as possible at two different levels. The acquired images had distinct grey-level histogram peaks for unhydrated cement particles, except for the unreacted ferrite phase which revealed a separate peak. Occasionally, a separate peak for CH and inner products appeared. The grey level for the ferrite phase (about 240) did not vary much, and was used for calibration. This was convenient because the ferrite phase hydrated slowly and had a fairly narrow grey-level peak. At these initial settings of brightness and contrast, the fractions of unreacted cement and ferrite phases were determined. The results of this part are reported in detail in [17]. The exact boundary of the pores, however, could not be distinguished very well. To overcome this problem, the image was collected a second time at a higher brightness setting while the contrast was appropriately corrected. A major effect of this operation was to expand the number of grey levels of the reaction products and pores. This made it possible clearly to distinguish distinct pores (i.e. hollow shells) from the groundmass [6] portion of reaction products. Nevertheless, distinct histogram peaks for larger pores could generally not be obtained because of diffuse boundaries between C–S–H and pores and because of backscattering of electrons from the bottom of shallow pores.

A binary segmentation process was used to determine the hollow-shell porosity. Based on the grey-level histogram, an initial threshold for the grey level corresponding to larger pores was set by judgement. The pixels corresponding to the grey level interval, from zero to this initial threshold value, were given a particular colour code and superimposed on the binary image. This was then visually checked to see if the coloured phase matched the pores in the black-and-white monitor image. This visual comparison was also made at a higher magnification, revealing somewhat smaller pores and more detailed pore boundaries. The painted digital image was also continuously compared against the image on the CRT monitor. The threshold grey level was corrected until the pores were satisfactorily covered by the coloured phase. Based on the final corrected grey-level threshold, the number of pixels corresponding to the grey-level range from zero and up to this threshold and relative to the total number of pixels in the image was taken as the area of larger pores. Because cement paste (without segregation) is considered to be an isotropic material, an area fraction is an estimate of the volume fraction. Thus, the percentage of pores larger than approximately 1 μm was estimated in this way. The procedure resulted in apparently consistent and repeatable results.

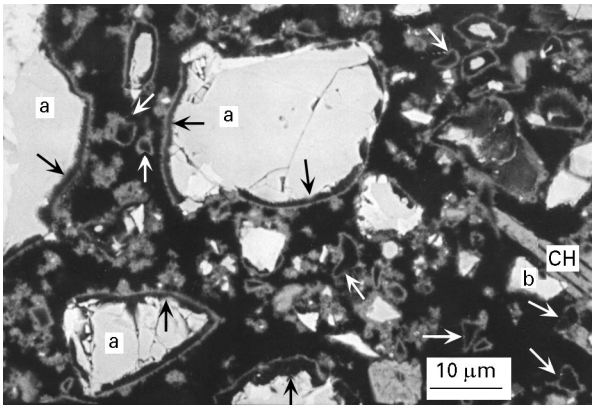

Figure 1 BSE image of the 0.55 w/b ratio paste, hydrated for 1 d. a, alite; b, belite; black arrows denote partially hollow shells while white arrows denote completely hollow shells.

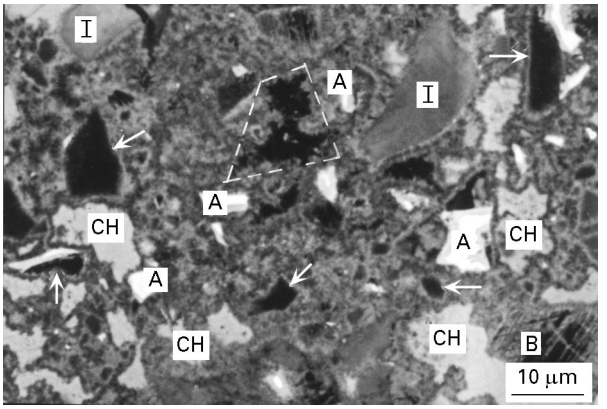

Figure 2 BSE image of the 0.55 w/b ratio paste, hydrated for 9 mon. I, inner product phase of C–S–H; A, ferrite/CH; B, hydrated belite; white arrows denote completely hollow shells.

3. Results

3.1. Characteristics of hollow shells

Fig. 1 shows a BSE image of the 0.55 w/b ratio paste hydrated for 1 d. The cement grains appear almost white, CH appears light grey, C–S–H appears generally as darker grey while pores appear black. At the age of 1 d, the extensive capillary pore system of the 0.55 w/b ratio paste is observed clearly. "Shells" of reaction products are seen at some distance around alite (a) particles while they appear to be in contact with belite (b) grains. The intra-shell separation of some of the partially hollow shells with remnant cement cores are marked with black arrows. While the larger alite grains form hollow shells with remnant anhydrous cores, many of the smaller cement grains (particularly alite and aluminate) hydrate completely by 1 d [11, 13], leaving completely hollow shells. Some completely hollow shells are marked with white arrows in Fig. 1. We have shown in a previous paper [14] that most of the smaller cement grains observed at the early age of 12 h had fully reacted by 1 d and left completely hollow shells, with the same size and shape as the unreacted smaller cement grains observed at 12 h. It should be noted that three-dimensional interpretation of two-dimensional images of flat polished specimens can occasionally be misleading. It is possible that some of the apparently hollow shells are the bottom or top of larger partially hollow shells.

"Shells" of reaction products form around alite grains, with an intra-shell void separating the shell of reaction products and receding anhydrous core. After 1 d at the high w/b ratio, the capillary porosity is so high that the shells of reaction products are clearly outlined (Fig. 1). At lower w/b ratios, the shell of reaction products may, from a physical point of view, virtually disappear through intergrowth of hydrates in the capillary pore space, i.e. outer products [14]. However, the void within the shell of outer reaction products is, literally, still termed "a hollow shell". Such an intergrowth of hydrates in the capillary pore space will also continue with age, thus physically distinct shells of reaction products observed at early ages may "disappear" at later ages as a result of continued deposition of outer products. This is seen from Fig. 2, which shows a BSE image of the 0.55 w/b ratio paste hydrated for 9 mon. The hydration has continued with deposition of outer products, and inner products. Some of the hollow shells containing remnant anhydrous cores at 1 d have apparently developed into completely hollow shells at 9 mon; some of these large completely hollow shells are marked with white arrows. The largest completely hollow shells are up to 10 μm across. The size and distinct shape of the voids indicate that they are relicts of cement grains. Capillary pore space is also outlined in Fig. 2.

Although some hollow shells remain after 9 mon hydration in this specimen, it is also clear that inner products have been formed extensively. Inner product phases of essentially C–S–H are marked with an "I" in Fig. 2. The texture of these C–S–H inner product phases appears much more homogeneous than the outer product phases consisting of mainly C–S–H; their size and shape indicate that they have formed within the original cement grain boundaries. The microstructural features marked "A" in Fig. 2 show remnant ferrite phases as the brightest areas and CH as the somewhat darker phases. The lower right partially hollow shell "B" is probably the remnant of a hydrated belite grain, which is indicated by the striated structure. Apparently, at later ages, belite grains may also hydrate according to a through-solution mechanism with the formation of hollow shells. This is also observed from Fig. 3 which shows a BSE image of the 0.40 w/b ratio paste, without csf, hydrated for 9 mon. The outlined striated partially hollow shell "B" is presumably a hydrated belite grain as indicated by the striated structure and size and shape of feature. EDX analysis showed the upper part to consist of C–S–H, while the brighter, more porous lower part is essentially CH. The phenograins [6] "I", contain inner products of C–S–H (darker phases) and CH (brighter phases). Several CH crystals, which probably have formed in previously formed hollow shells, are marked with black crosses. The white crosses denote AFm phases, also presumably formed in previously formed hollow shells. Formation of CH and AFm in previously established hollow shells will be discussed later.

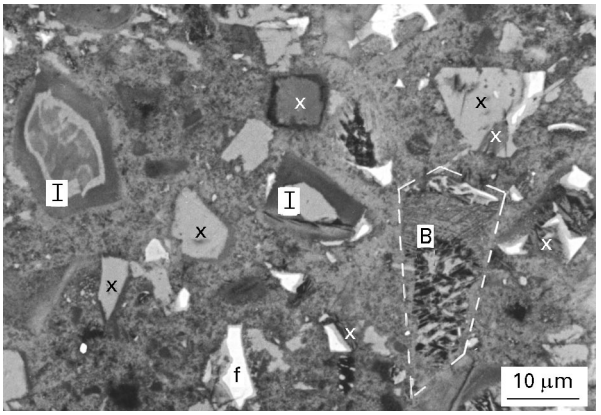

Figure 3 BSE image of the 0.40 w/b ratio paste, without silica fume, hydrated for 9 mon. f, ferrite; I, inner product phase of C–S–H/CH; B, hydrated belite; black and white crosses denote CH and AFm phases, respectively.

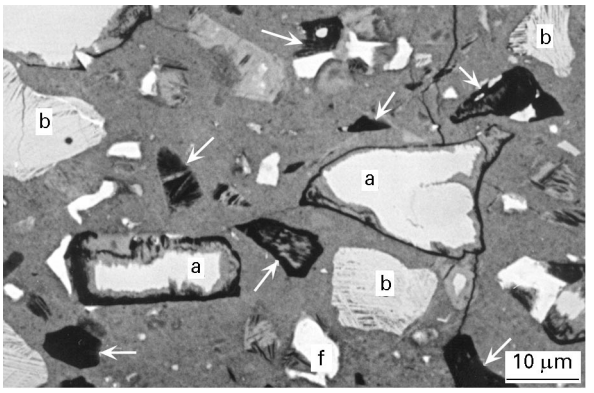

Figure 5 BSE image of the 0.25 w/b ratio paste, with silica fume, hydrated for 9 mon. a, alite; b, belite; f, ferrite; arrows denote completely hollow shells.

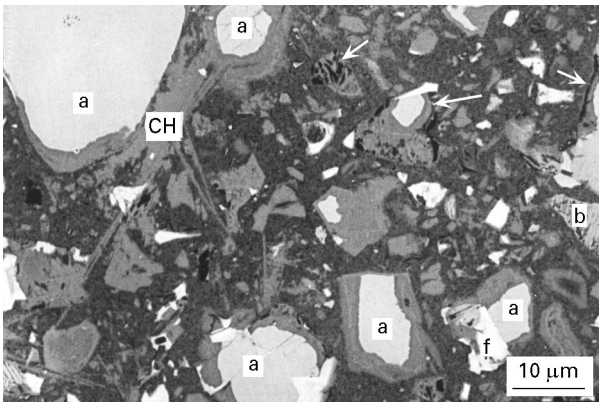

Figure 4 BSE image of the 0.25 w/b ratio paste, without silica fume, hydrated for 9 mon. a, alite; b, belite; f, ferrite; arrows denote partially hollow shells.

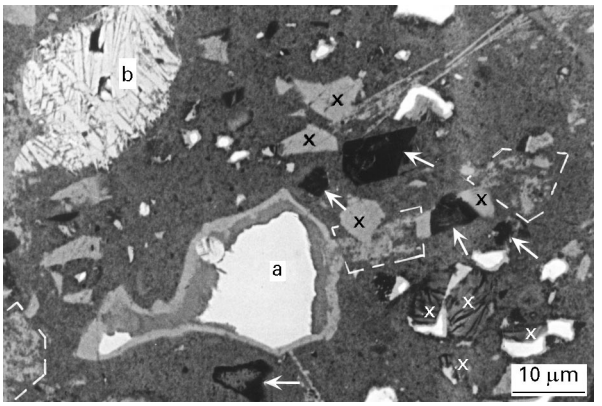

Figure 6 BSE image of the 0.30 w/b ratio paste, with silica fume, hydrated for 9 mon. From 1–9 mon this specimen was water cured. a, alite; b, belite; arrows denote hollow shells; black and white crosses denote CH and AFm phases, respectively.

Fig. 4 depicts an area of the 0.25 w/b ratio paste, without csf, hydrated for 9 mon. Relatively few hollow shells are observed; some of the partially hollow shells are marked with arrows. The specimen of the same mix hydrated for 1 d was previously shown in [14]. Between 1 d and 9 mon, inner products form extensively. The hollow shells observed at 1 d have largely been refilled with fresh hydration product, mainly C–S–H, but also CH and AFm.

Fig. 5 shows a BSE image of the 0.25 w/b ratio paste, containing csf, after 9 mon hydration. Several completely, or nearly completely hollow shells are observed. Some of these are marked with arrows. This mix contains many more hollow shells than the 0.25 w/b ratio paste without csf (Fig. 4). It is apparent that the formation of inner products at somewhat later ages is less favoured in the mixes containing csf. The microstructure of this 0.25 w/b ratio paste hydrated for 1 d was discussed elsewhere [14].

Fig. 6 shows a BSE image of the 0.30 w/b ratio paste, containing csf, after 9 mon hydration. This specimen was water-cured between 1 and 9 mon. Some nearly completely hollow shells are marked with arrows. Large AFm phases are marked with white crosses. Unreacted ferrite phases and some CH are observed in relation to these AFm phases. These AFm phases have presumably deposited in previously formed partially hollow shells containing some remnant anhydrous ferrite. Around the large alite (a) core in the central part of the image, inner products of C–S–H (darker grey) and CH (brighter grey) have formed. Several CH crystals appear to have formed in established hollow shells as was also seen in Fig. 3; some of these are marked with black crosses. The size and shape of the CH indicate that they have deposited in previously formed hollow shells. The CH observed in the outer product phase have generally no distinct shape, but appear intermixed with C–S–H, probably due to the pozzolanic reaction. Some of the areas containing intermixed CH/C–S–H in the outer product phase are outlined in Fig. 6.

3.2. Quantity of hollow shells – hollow-shell porosity

The image analysis procedure was used to measure the quantity of hollow shells. The quantity of hollow shells expressed as per cent porosity is given in Fig. 7. For the pastes of 0.30 w/b ratio or below, the quantity of hollow shells could be measured from 1 d. A

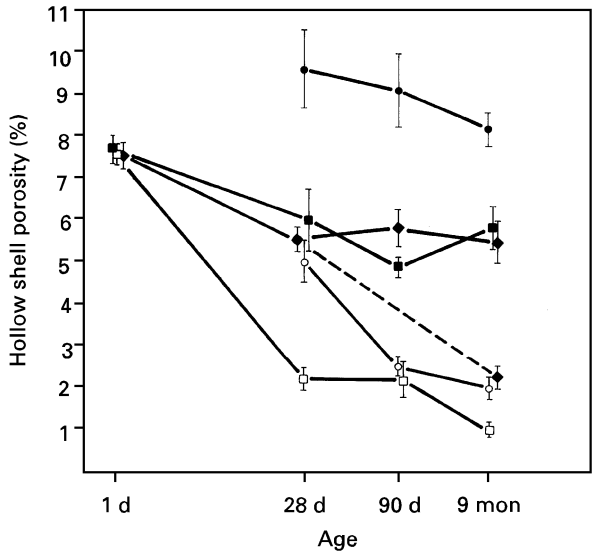

Figure 7 Volume of hollow shells in relation to paste volume (i.e. hollow-shell porosity) versus curing time. Mean values with standard deviation. w/b ratio: (□) 0.25, (■) 0.25/10% csf, (–◆–) 0.30/5% csf, (– –◆– –) 0.30/5% csf wet cured, (○) 0.40, (●) 0.40/10% csf.

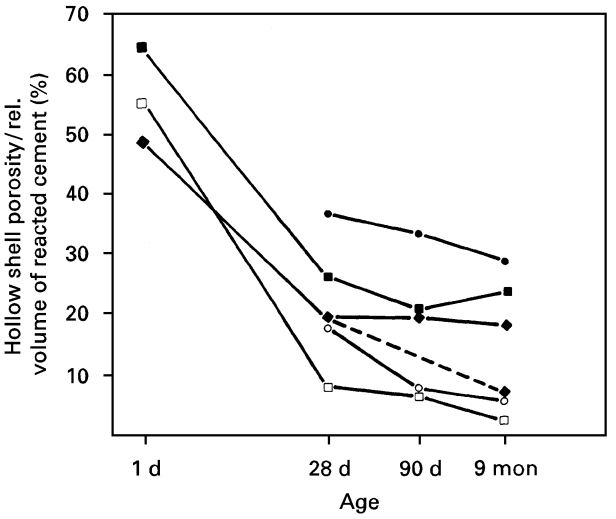

Figure 8 Hollow-shell porosity divided by the specific volume of reacted cement versus curing time (i.e. the hollow-shell porosity is divided by the volume of reacted cement relative to the paste volume). w/b ratio: (□) 0.25, (■) 0.25/10% csf, (–◆–) 0.30/5% csf, (– –◆– –) 0.30/5% csf wet cured, (○) 0.40, (●) 0.40/10% csf.

detailed examination of a low w/b ratio paste hydrated for 12 h [14] revealed that it practically contained almost no pores larger than about 1 μm. Hollow shells were not apparent at 12 h for this mix. Capillary pores become smaller with continued hydration, while hollow shells develop simultaneously. Thus, there is no possibility that capillary pores will be included in the image analysis after 1 d in the low w/b ratio pastes. For similar reasons, with the 0.40 w/b ratio pastes, the quantity of hollow shells were measured for samples 28 d and older. The quantification of hollow shells was complicated by the presence of capillary pores for the 0.55 w/b ratio paste at all ages (Fig. 2), and consequently, this mix was not analysed. The hollow-shell pores have not been intermixed with other types of voids.

It can be observed from Fig. 7 that the quantity of hollow shells generally decreases with increasing age and decreasing w/b ratio. Water-curing appears to decrease the hollow-shell porosity. At later ages, the mixes containing csf have much greater percentages of hollow-shell pores than mixes without csf. The 0.25 and the 0.40 w/b ratio pastes with 10% csf has, at later ages, a hollow-shell porosity of about 5.5% and 9%, respectively. Based on data of Sellevold [18], the total porosity would be expected to be about 30% and 40% for the two respective mixes. If we assume that hollow shells are included in these estimates, hollow shells constitute about 20% of the total porosity in these mixes.

The significance of hollow shells can also be seen from Fig. 8, where the hollow-shell porosity is relative to the specific volume of reacted cement, i.e. the hollow-shell porosity is divided by the volume of reacted cement relative to the total paste volume. Fig. 8 shows the fraction of hydrated cement, at a particular age, which has hydrated in a manner resulting in hollow shells. It can be observed from Fig. 8 that at 1 d, between about 50% and 65% of the reacted cement has left hollow shells. At later ages, it appears that more of the reaction occurs with the formation of inner products. Even at 28 days, at least 40% of the reacted cement has left hollow shells in the 0.40 w/b ratio paste containing csf. It should be noted that the relation between the hollow-shell porosity and the relative volume of reacted cement may underestimate the fraction of cement hydrated so as to leave hollow shells, as previously formed hollow shells may later become filled with fresh hydrates. It has been suggested that CH may dissolve, and leave "apparent hollow shells", due to the pozzolanic reaction with csf [19]. We have not observed this in our work, and the higher hollow-shell porosity at later ages observed in the specimens containing csf (Figs 4–8) is due to a reduced formation of fresh reaction products within the original cement grain peripheries. Our results indicate that the pozzolanic reaction largely is an *in situ* reaction (Fig. 6).

4. Discussion

Early in the hydration process, a rim of reaction products, probably composed of C–S–H and AFt [11, 13], form on the cement grain surfaces. As the cement grains recede due to further hydration, stable hydrates no longer seem to form to any large extent within the original cement grain boundaries up to the age of 1 d. Rather, the cement appears to hydrate according to a through-solution mechanism with the formation of hollow shells. Formation of hydrates generally occurs in the capillary pore space, i.e. as outer products. The rim of reaction products mostly grows outward in the capillary pore space by deposition of outer products. Hollow-shell hydration appears to be a dominant hydration mode up to the age of approximately 1 d, as indicated by Figs 1 and 8 of this paper and Figs 4 and 5 of [14]. In this study, hollow shell formation was only seen in relation to the hydration of alite up to 1 d.

The shells of reaction products were separated from the receding anhydrous alite phases by considerable intra-shell space. At later ages, outer products continue to form, while simultaneously, inner products are also formed. This implies, in particular, that those partially hollow shells, with remnant anhydrous cores present earlier in the hydration process, may later become filled with fresh hydration products, mainly C–S–H. The completely hollow shells formed earlier in the hydration may remain empty at later ages, or may be refilled with fresh hydrates, mainly CH and AFm presumably. The resulting effect is a general decrease in hollow-shell porosity at later ages (Fig. 7).

At early ages, hollow shells were never observed in relation to belite phases, probably because very little belite has hydrated by 1 d. There was close contact between the phase of hydrates and anhydrous phase. Hollow-shell hydration was observed, however, in relation to belite at 9 mon. The striated structure of many belite grains becomes apparent in BSE images at later hydration ages as the lamellae containing more reactive anhydrous material may or may not be replaced by product. Apparently, hydrates may form *in situ* or the dissolved anhydrous species may migrate away, leaving a partially hollow shell with a characteristic striated structure (Figs 2–6).

Different types of porosity are present in cement-based materials: gel pores, capillary pores and hollow-shell pores. Voids may also result from processing due to bleeding or insufficient compaction. "Processing pores", when they are present, have different characteristics from hollow-shell pores. They do not have the size or shape of cement grains and they do not contain remnant anhydrous cores, for example. The hollow shells we have presented here and elsewhere [14] result from a hollow-shell hydration mode. In the 0.25 w/b ratio paste we examined earlier [14], we showed that hollow-shell pores were apparent at 1 d, but not at 12 h. The hollow-shell voids observed at 1 d were substantially larger than any of the pores observed at 12 h hydration. As these voids do not result from the preparation of the specimens [14, 15], they provide direct evidence that larger voids can result from hydration. If they had been any other type of void, for instance entrapped air-voids or bleeding pores, they would also have been observed at 12 h, but were not.

Capillary pores change with time by the precipitation of hydrates, mainly C–S–H, in the originally water-filled space. These precipitation processes and the nature of C–S–H leads to an extremely disordered physical structure, the surface of which are the boundaries of the gel- and capillary pores. Hollow shells, on the other hand, are usually regular and closed and generally have a distinct shape of the relicts of cement particles. When they are partially filled with hydrates, their physical structure might be complex. Small hollow shells formed during early ages, and which later may be filled with hydrates, can be difficult to characterize. These hydrates would, strictly speaking, be inner products, although, due to experimental problems, they may incorrectly be characterized as outer products. For this reason, Taylor [20] abandoned the term "outer product", and suggested the term "undesignated product" to comprise outer products and indistinguishable inner products. Anyway, while capillary pores generally are part of a very disordered pore system, hollow shells are, by comparison, generally very distinct. It is therefore, generally not a problem to differentiate between the two by electron microscopy. At somewhat later ages and lower w/b ratios, hollow shells can be larger than capillary pores by more than two orders of magnitude. Traditionally, the intrinsic pores of cement hydration have been considered to be comprised of both gel- and capillary pores. Based on this work and previous reports [6–14], hollow shells can be considered to be a third type of intrinsic pore of cement hydration, along with gel and capillary pores.

CH and large AFm phases are frequently observed to have formed in hollow shells. This was particularly observed in the water-cured 0.30 w/b ratio specimen (Fig. 6), and is partly responsible for the reduced hollow-shell porosity of this specimen (Figs 7 and 8). The water-curing did promote the hydration of the ferrite phase considerably [17], which may have increased the formation of AFm. Large AFm phases, often many micrometres across (Fig. 6), were never detected at relatively early ages (1 d), and because they are much larger than any pores or voids initially present in the low w/b ratio pastes at this relatively early age, except for hollow shells, they must have formed in the hollow shells. This presumably implies that sulphate can migrate into the hollow shells and form AFm. The large AFm phases were especially observed in the 0.55 and 0.40 w/b ratio pastes cured in a sealed container and in the water-cured 0.30 w/b ratio paste, and not so frequently in the low w/b ratio pastes allowed to self-desiccate. It has been hypothesized that AFm may deposit in hollow shells [21, 22]. The formation of CH, AFm, and possibly AFt, at relatively late ages in previously formed hollow shells is similar to the well-known formation of these phases in water-saturated cracks or air-voids. Crystal growth preferably occurs in larger spaces [23].

5. Conclusion

The microstructural development of cement paste formulations of ordinary and high-performance concrete have been studied by electron microscopy and image analysis. The binder was comprised of a low-alkali sulphate-resistant cement and silica fume. The characteristics and quantities of hollow shells (Hadley grains) have been studied extensively. At later ages, the hollow-shell porosity varied between 1% and 9% depending on mix composition and curing regime. The presence of silica fume increased the hollow-shell porosity considerably, while the hollow-shell porosity generally decreased with decreasing w/b ratios in the range of 0.40–0.25. Hollow shells were estimated to constitute approximately 20% of the total porosity in those mixes containing 10% silica fume, and about 10% or less in the mixes without silica fume.

Water-curing reduced the hollow shell porosity at later ages.

Acknowledgements

We acknowledge the financial support provided by the Foundation for Swedish Concrete Research of the Swedish research consortium of high-performance concrete structures. The latter group consists of Cementa, Elkem Materials, Euroc Beton, NCC, Skanska, Strängbetong, and the government authorities BFR and Nutek. We would also like to thank Nora Dahle who assisted in the microscopy.

References

1. J. H. TAPLIN, Austr. J. Appl. Sci. **10** (1959) 329.
2. T. C. POWERS, *J. PCA Res. Devel. Lab.* **3** (1961) p. 47 (Portland Cement Association, Skokie).
3. G. VERBECK, "Bulletin 197", PCA Research and Development Laboratories (Portland Cement Association, Skokie, 1966).
4. S. DIAMOND, in "Proceedings of a Conference on Hydraulic Cement Pastes and Their Structure and Properties" (Cement and Concrete Association, London, 1976) p. 2.
5. H. M. JENNINGS, B. J. DALGLEISH and P. L. PRATT, *J. Am. Ceram. Soc.* **64** (1981) 567.
6. S. DIAMOND and D. BONEN, *ibid.* **76** (1993) 2993.
7. D. W. HADLEY, PhD thesis, Purdue University, USA (1972).
8. B. D. BARNES, S. DIAMOND and W. L. DOLCH, *Cem. Concr. Res.* **8** (1978) 263.
9. B. J. DALGLEISH, P. L. PRATT and E. TOULSON, *J. Mater. Sci.* **17** (1982) 2199.
10. P. L. PRATT and A. GHOSE, *Philos. Trans. R. Soc. Lond.* **A310** (1983) 93.
11. K. L. SCRIVENER and P. L. PRATT, *Proc. Br. Ceram. Soc.* **35** (1984) 207.
12. K. O. KJELLSEN, R. J. DETWILER and O. E. GJØRV, *Cem. Concr. Res.* **21** (1991) 179.
13. K. L. SCRIVENER, in "Materials Science of Concrete", Vol. 1, edited by J. Skalny (The American Ceramic Society, Westerville, OH, 1989) p. 127.
14. K. O. KJELLSEN, H. M. JENNINGS and B. LAGERBLAD, *Cem. Concr. Res.* **26** (1996) 593.
15. K. O. KJELLSEN and A. MONSØY, in "Proceedings of the 18th International Conference on Cement Microscopy", edited by L. Jany, A. Nisperos and J. Bayles (International Cement Microscopy Association, Duncanville, 1996) p. 356.
16. K. O. KJELLSEN, H. M. JENNINGS and B. LAGERBLAD, to be submitted.
17. K. O. KJELLSEN, L. FJÄLLBERG and T. SKJETNE, CBI report, Swedish Cement and Concrete Research Institute, Stockholm, 1977, in press.
18. E. SELLEVOLD, in "SINTEF report STF70A92050" (SINTEF Civil and Environmental Engineering, Trondheim, 1992) in Norwegian.
19. D. P. BENTZ and P. E. STUTZMAN, *Cem. Concr. Res.* **24** (1994) 1044.
20. H. F. W. TAYLOR, *Adv. Cem. B. Mater.* **1** (1993) 38.
21. K. O. KJELLSEN and R. J. DETWILER, in "Proceedings of the 9th International Congress on the Chemistry of Cement", Vol. 4 (National Council for Cement and Building Materials, New Delhi, 1992) p. 241.
22. K. L. SCRIVENER and H. F. W. TAYLOR, *Adv. Cem. Res.* **5** (1993) 139.
23. V. JOHANSEN, N. THAULOW and J. SKALNY, Betonw. Fertigt. Techn. **62/11** (1995) 56.

Received 8 May 1996
and accepted 7 January 1997